

## Supplement materials

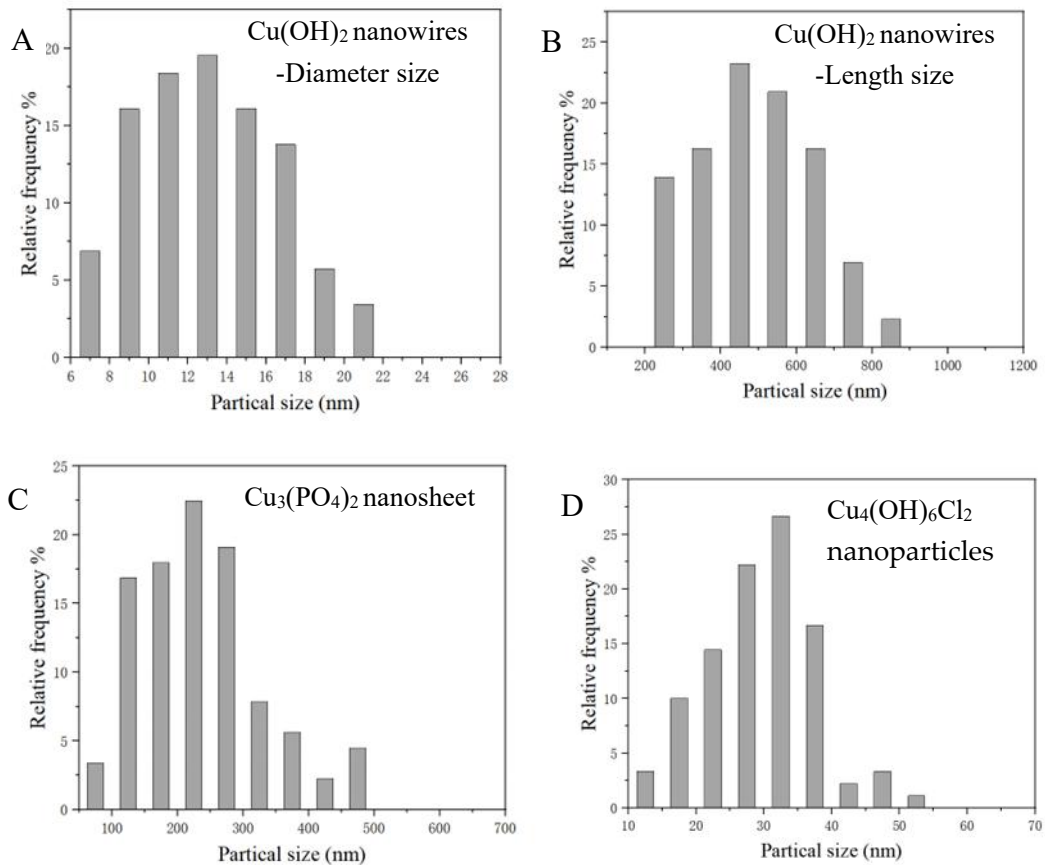


Figure S1. Size distribution of three kinds of copper-based nanoparticles. A. Cu(OH)<sub>2</sub> nanowires diameter statistical histogram; B. Cu(OH)<sub>2</sub> nanowires length statistical histogram; C. Histogram of length statistics of Cu<sub>3</sub>(PO<sub>4</sub>)<sub>2</sub> nanosheets; D. Histogram of Cu<sub>4</sub>(OH)<sub>6</sub>Cl<sub>2</sub> Nanoparticle Size Statistics.

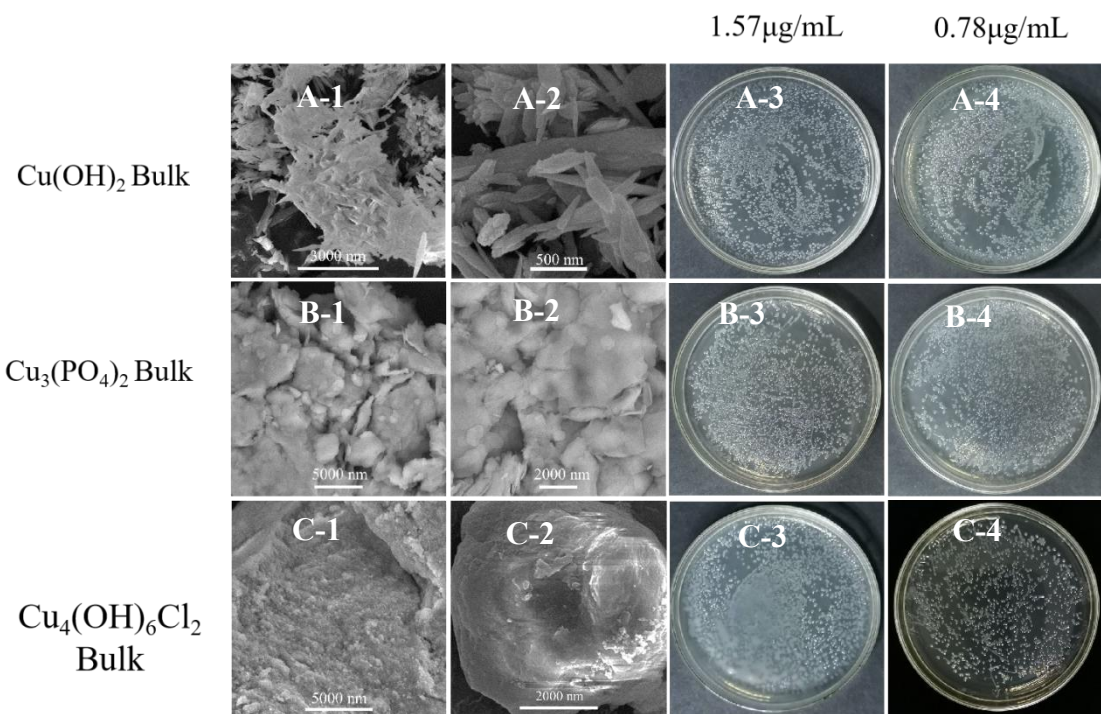


Figure S2. Characterization(A, B, C) of commercial copper-based compounds  $\text{Cu}(\text{OH})_2$ ,  $\text{Cu}_3(\text{PO}_4)_2 \cdot 3\text{H}_2\text{O}$ , and  $\text{Cu}_4(\text{OH})_6\text{Cl}_2$  and their inactivation efficiency( $\text{Cu}(\text{OH})_2$ : A-3, A-4;  $\text{Cu}_3(\text{PO}_4)_2 \cdot 3\text{H}_2\text{O}$  : B-3, B-4,  $\text{Cu}_4(\text{OH})_6\text{Cl}_2$ : C-3, C-4) of Psa.

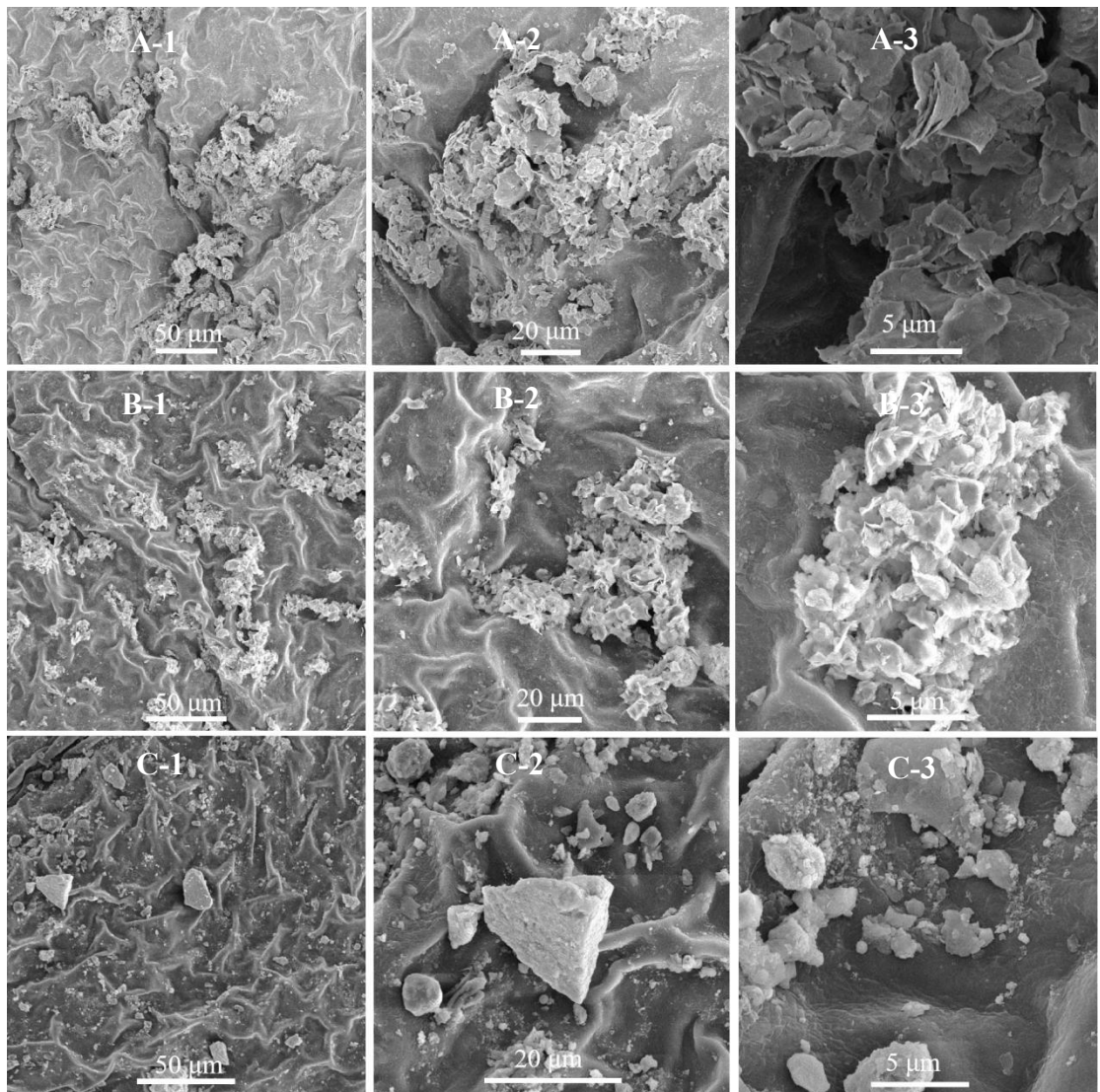


Figure S3. The distribution of three kinds of commercial copper-based compounds on the surface of kiwifruit leaves. A. Bulk Cu(OH)<sub>2</sub>; B. Bulk Cu<sub>3</sub>(PO<sub>4</sub>)<sub>2</sub>; C. Bulk Cu<sub>4</sub>(OH)<sub>6</sub>Cl<sub>2</sub>.

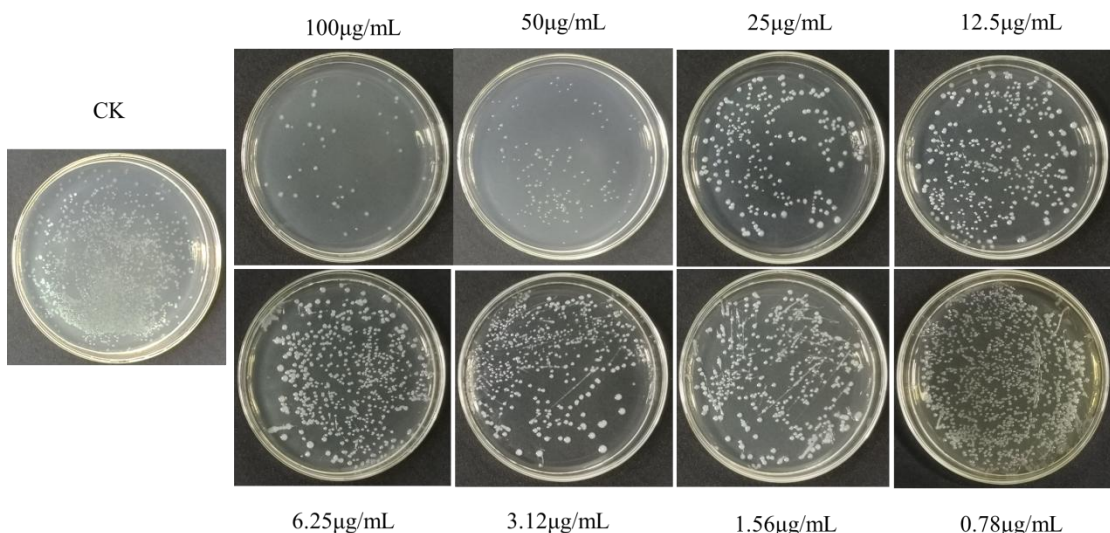


Figure S4. The MBC of the positive control agent thiadiazole copper.

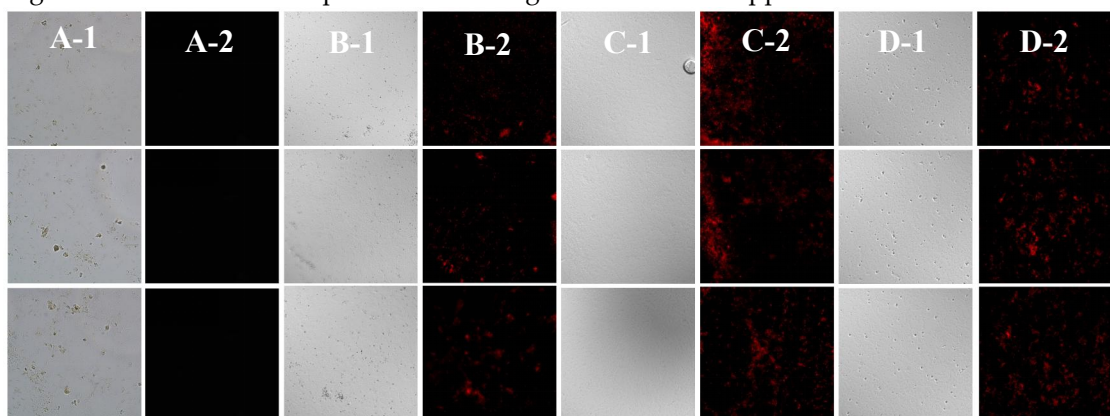


Figure S5. Supplementary fluorescence images for the membrane permeability test of Psa . A-1, B-1, C-1, D-1 bright field image; A-2, B-2, C-2, D-2 dark field image;Thiodiazole copper(A-1,A-2), $\text{Cu(OH)}_2$  nanowires (B-1, B-2),  $\text{Cu}_3(\text{PO}_4)_2\cdot 3\text{H}_2\text{O}$  nanosheets (C-1, D-2) and  $\text{Cu}_4(\text{OH})_6\text{Cl}_2$  nanoparticles (C-1, D-2).

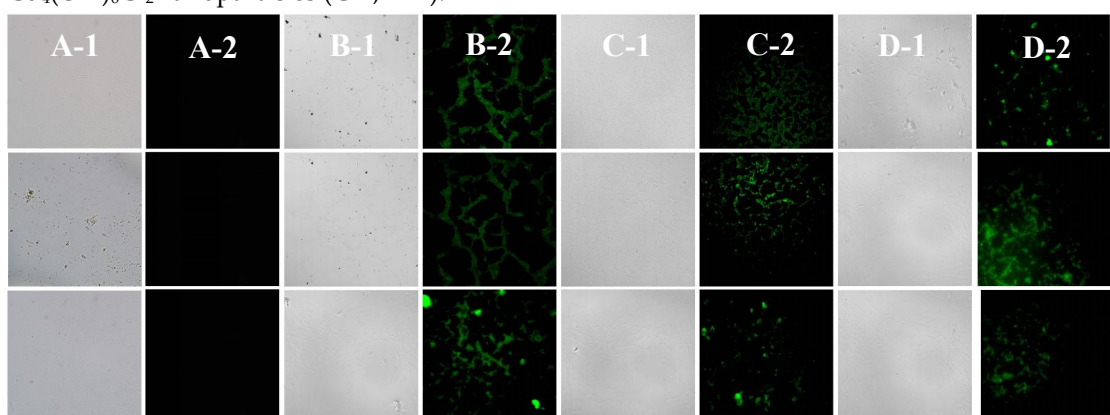


Figure S6. Supplementary fluorescence image for reactive oxygen species (ROS) accumulation test of Psa. A-1, B-1, C-1, D-1 bright field image; A-2, B-2, C-2, D-2 dark field image; Thiodiazole copper(A-1,A-2), $\text{Cu(OH)}_2$  nanowires (B-1, B-2),  $\text{Cu}_3(\text{PO}_4)_2\cdot 3\text{H}_2\text{O}$  nanosheets (C-1, D-2) and  $\text{Cu}_4(\text{OH})_6\text{Cl}_2$  nanoparticles (C-1, D-2).

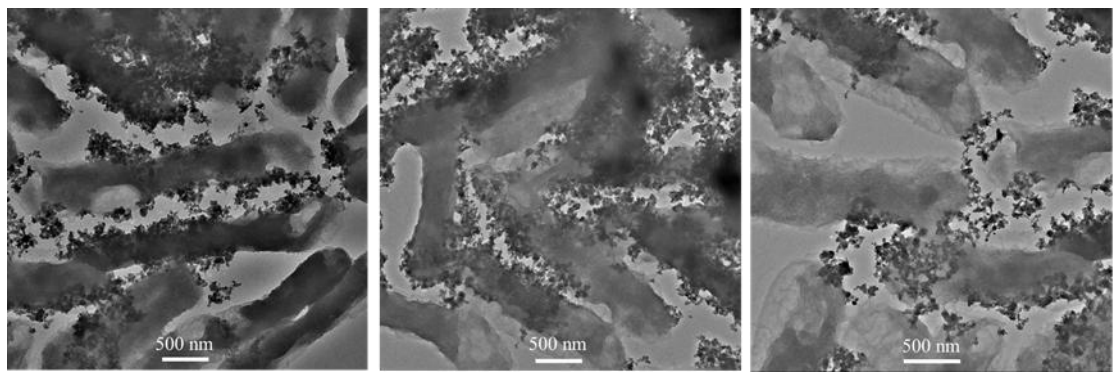


Figure S7. Supplementary TEM images for the interaction between Psa and Cu<sub>4</sub>(OH)<sub>6</sub>Cl<sub>2</sub> nanoparticles.

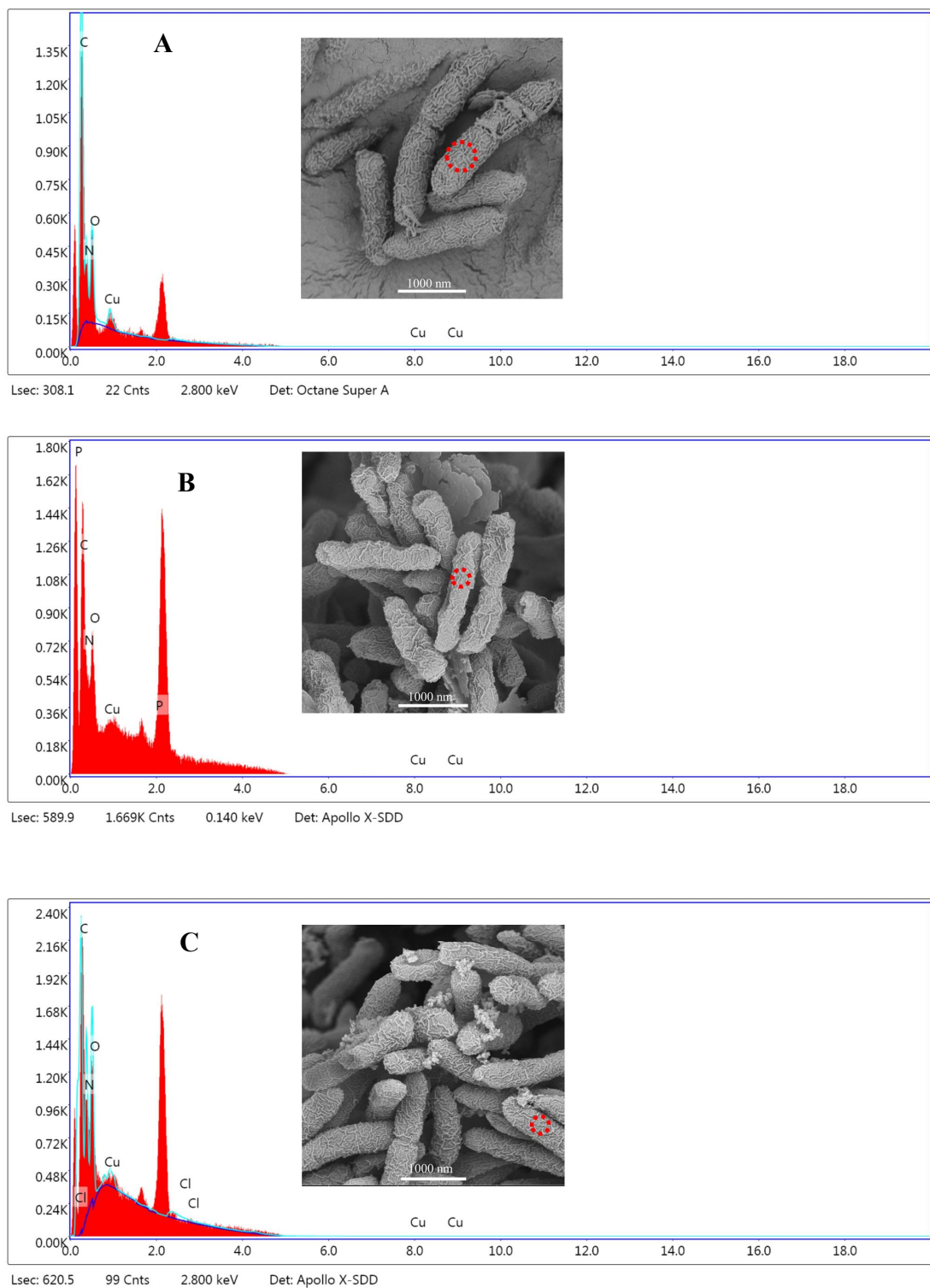


Figure S8. Supplementary SEM images and EDS spectrogram for the interaction between Psa and nanoparticles. A.  $\text{Cu}(\text{OH})_2$ ; B.  $\text{Cu}_3(\text{PO}_4)_2$ ; C.  $\text{Cu}_4(\text{OH})_6\text{Cl}_2$ .

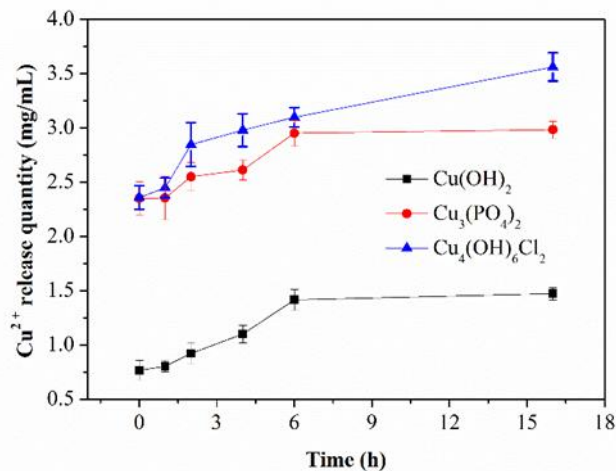


Figure S9. Concentration of Cu<sup>2+</sup> in solution vs time after the indicated nanomaterials was introduced into aqueous solution at a mass concentration of 200 µg/mL.

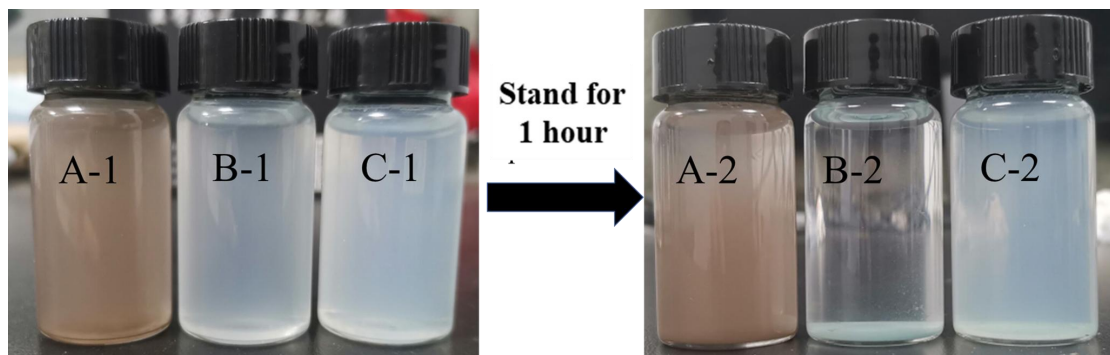


Figure S10. Colloidal stability test of copper-based nanoparticles dispersion. A. Cu(OH)<sub>2</sub>; B. Cu<sub>3</sub>(PO<sub>4</sub>)<sub>2</sub>; C. Cu<sub>4</sub>(OH)<sub>6</sub>Cl<sub>2</sub>.

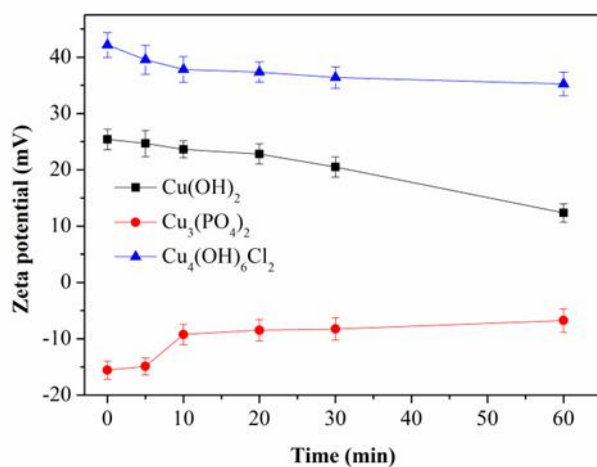


Figure S11. Zeta potential vs time of nanomaterials solution at a mass concentration of 200 µg/mL.